Partition between the fission fragments of the excitation energy and of the neutron multiplicity at scission in low-energy fission

N. Carjan,[1,2] F.-J. Hambsch,[1] M. Rizea,[2] and O. Serot[3]
[1]*EC-JRC, Institute for Reference Materials and Measurements, B-2440 Geel, Belgium*
[2]*Horia Hulubei-National Institute for Physics and Nuclear Engineering, P.O. Box MG-6, RO-077125 Magurele, Romania*
[3]*CEA Cadarache, F-13108 Saint Paul lez Durance, France*
(Received 19 August 2011; revised manuscript received 4 January 2012; published 2 April 2012)

The partition between the light (L) and the heavy (H) fission fragments of the excitation energy available at scission is studied in the framework of the sudden approximation, i.e., under the assumption that the neck rupture and the absorption of the neck pieces by the fragments happen infinitely fast. We are dealing with a sudden transition between two different nuclear configurations ($\alpha_i \rightarrow \alpha_f$) and we only need to know the two sets of neutron eigenstates involved. The accent in the present work is put on the dependence of this share of energy on the mass asymmetry A_L/A_H of the primary fission fragments during the low-energy fission of ^{236}U. In particular, for every fragment mass A we estimate the scission neutron multiplicity ν_{sc}, the average energy cost for their release $\langle E_{\nu sc}\rangle$, the primary fragments' excitation energy E^*_{sc}, and the corresponding temperature T_{sc}. The results are analyzed separately for each value of Ω (the projection of the angular momentum on the symmetry axis). As general trends, a decrease of E^*_{sc} (T_{sc}) and an increase of ν_{sc} ($\langle E_{\nu sc}\rangle$) with increasing A were observed.

DOI: 10.1103/PhysRevC.85.044601 PACS number(s): 25.85.Ec, 02.60.Lj, 02.70.Bf, 24.75.+i

I. INTRODUCTION

The partition of the total excitation energy (TXE) between the light (L) and the heavy (H) fragments is essential for the simulation of the neutron evaporation and of the γ-ray emission from fully accelerated fragments. In turn, the study of these two modes of fragment deexcitation plays an important role in the fundamental understanding of the nuclear fission process as well as in its applications.

Because there is no theoretical approach and no way to determine this energy partition from the experimental data, arbitrary hypotheses have been adopted so far [1–7]. A simple law for the ratio of the nuclear temperatures T_L/T_H as a function of the mass ratio A_L/A_H was usually assumed: either a constant or a linear dependence. In Ref. [7] this ratio was obtained by minimization of the discrepancy with experimental data for each mass division.

TXE has three main terms: E^*_{sc}, the intrinsic excitation energy of the primary fragments immediately after scission (which may or may not have a prescission contribution); the unknown fraction of $E_{\nu sc}$, the energy used to release neutrons during scission, which corresponds to the partial reabsorption of these neutrons by the fragments; and ΔE_{def}, the extra deformation energy, i.e., the difference between the deformation energy of the fragments immediately after scission and that of the fragments in their ground states. In view of the different origins of these three terms, it is inconceivable that a single simple rule governs their sharing between the two fragments. In addition no thermal equilibrium can be asssumed for ΔE_{def} because it is defined when the fragments are no longer in contact and it is transformed into internal heat when the fragments are well separated. Within the limited shape parametrization (only one degree of freedom for each mass asymmetry) of the present study, ΔE_{def} is totally constrained and other normal modes cannot be included.

There is a consensus that a more fundamental approach to the partition of the excitation energy at scission is needed. A microscopic scission model for the transition from two fragments connected by a thin neck (α_i) to two separated fragments (α_f) was recently developed [8]. It is based on the sudden approximation [9] that assumes that this transition happens infinitely fast. The sudden change of the potential in which the nucleons move produces, by means of an extremely diabatic coupling, their excitation and eventual emission. This is the main source of fragments' excitation at α_f if we assume the system to be relatively cold at α_i. This assumption is supported by dynamical calculation [10] of the coupling between the nucleonic degrees of freedom and the rapidly changing potential during the descent from saddle to scission using the time-dependent Schrödinger equation with time-dependent potential. It indicates that for descent times around 5×10^{-21} s the single-particle excitations are smaller than a typical neutron separation energy ($\approx$6 MeV). For larger, more realistic, saddle-to-scission times this excitation tends to zero.

This argument is however model dependent and two-body effects may lead to a finite prescission excitation energy. In the present formalism it is easy to include the effect of a nonzero temperature in the prescission configuration by modifying the occupation probabilities (see Sec. II). Therefore our assumption that the system is initially cold should be regarded as a working, but not crucial, hypothesis.

The model from Ref. [8] was used to calculate E^*_{sc} and $E_{\nu sc}$ as a function of the mass asymmetry of the fission fragments in the ^{235}U(n_{th}, f) reaction [11]. The results reported were integrated over both fragments. In the present work we continue this study and propose a simple way to separate the contributions of the L and H fragments to the excitation energy available at scission. It uses the probability of each excited (or emitted) neutron to be present in the L fragment or in the H fragment.

Another novel idea for this energy partition was proposed recently [12–14]: an entropy-driven accumulation of the

excitation energy in the heavy fragment. It is applicable to moderately excited (above the barrier) fissioning nuclei while our approach is applicable to low-energy fission (at and below the barrier).

The formalism used to calculate $E^*_{\rm sc}$ and $E_{\nu{\rm sc}}$ and their partition between the primary fission fragments is presented in Sec. II. Section III contains numerical results for ^{236}U as a function of each fragment's mass for the intrinsic excitation energy and the corresponding temperature, for the multiplicity of the unbound neutrons at scission, and for the average energy necessary to bring them into the continuum. Experimental indications about the excitation energy or the nuclear temperature at scission are also mentioned for comparison. Section IV is dedicated to a summary and conclusions.

II. THE SUDDEN APPROXIMATION

The sudden approximation is a stationary approach to the scission process. It only needs the two sets of bound-neutron eigenstates in the two nuclear configurations considered: $|\Psi^i(\alpha_i)\rangle$ and $|\Psi^f(\alpha_f)\rangle$. They are characterized by the projection Ω of the angular momentum on the symmetry axis. They are solutions of the bidimensional stationary Schrödinger equation for a neutron in the mean field of its interaction with the other nucleons. It is solved on a (ρ,z) grid and discretized by finite-difference approximations of the derivatives [15].

The nuclear shapes just before and immediately after scission are described by the rotation of two-parameter Cassini ovals around their symmetry axis [16,17]: ($\alpha_i = 0.985$, α_1^i) and ($\alpha_f = 1.001$, α_1^f), respectively. The first deformation parameter describes the elongation and the second the mass asymmetry. Note that $\alpha = 1.0$ describes a zero-neck scission shape. The value of the minimum neck radius (1.5 fm) is chosen in agreement with theoretical predictions along the dynamical path calculated with one-body dissipation [18]. Cassini ovals with such a neck radius are very close to the conditional maximal-deformation shapes, obtained by minimization of the deformation energy at fixed value of the distance between the centers of mass of the future fragments and at fixed mass asymmetry [19–21].

The formulas for $E^*_{\rm sc}$ and $\nu_{\rm sc}$ are deduced in Refs. [8,11] and summarized below. The excitation energy in which the fragments are left immediately after scission is given by

$$E^*_{\rm sc} = 2 \times \left(\sum_f V_f^2 e_f - \sum_f v_f^2 e_f \right), \tag{1}$$

where

$$V_f^2 = \sum_i v_i^2 |a_{if}|^2 \tag{2}$$

is the probability that an eigenstate $|\hat{\Psi}^f\rangle$ of the final configuration α_f is occupied after the sudden transition and e_f is its eigenenergy. The i and f sums are over the bound states of the initial and final nuclear configurations, respectively. Here $a_{if} = \langle \hat{\Psi}^i | \hat{\Psi}^f \rangle = 2\pi \int\int (g_1^i g_1^f + g_2^i g_2^f) d\rho dz$. The factor 2 represents the degeneracy of each state; g_1 and g_2 are the spin-up and spin-down components of $\hat{\Psi} = \rho^{1/2}\Psi$; and $v_{i,f}^2$ are the ground-state occupation probabilities of an eigenstate in the initial (α_i) and in the final (α_f) configuration, respectively. In the framework of the independent-particle model, $v_{i,f}^2$ are step functions: 1 for states below the Fermi level and 0 for states above the Fermi level. Possible correlations between neutrons will smooth this function. To include this effect in the calculated quantities, BCS occupation probabilities are used:

$$v_{i,f}^2 = \frac{1}{2} \left(1 - \frac{e_{i,f} - \lambda_{i,f}}{\sqrt{(e_{i,f} - \lambda_{i,f})^2 + \Delta_{i,f}^2}} \right). \tag{3}$$

A possible nonzero temperature at α_i produces the same smoothing of the step function. Therefore it could be easily taken into account in the present formalism. In fact the BCS occupation probabilities used are equivalent with a temperature of about 0.5 MeV.

The multiplicity of the unbound neutrons immediately after scission is given by

$$\begin{aligned} \nu_{\rm sc} &= 2 \times \sum_i v_i^2 \left(\sum_u |a_{iu}|^2 \right) \\ &= 2 \times \sum_i v_i^2 \left(1 - \sum_f |a_{if}|^2 \right). \end{aligned} \tag{4}$$

The i and the f sums are over bound states while the u sum is over unbound (continuum) states.

These neutrons are either emitted or reabsorbed by the fragments [22]. In the latter case, the average energy cost to release them,

$$\langle E_{\nu{\rm sc}} \rangle = \nu_{\rm sc} \times |\lambda_i|, \tag{5}$$

is redeposited in the fragments and subsequently used to evaporate neutrons and emit γvrays. In Eq. (5) we suppose that the average kinetic energy of the scission neutrons is close to zero and they initially lie around the Fermi level λ_i.

Finally we introduce the probabilities that each bound neutron (both in the α_i and in the α_f configurations) is present in the light (respectively, heavy) fragment:

$$N_{i,f}^L = 2\pi \int_0^R \int_{-Z}^{z_{\rm min}} \left[\left(g_1^{i,f}\right)^2 + \left(g_2^{i,f}\right)^2 \right] d\rho dz, \tag{6}$$

$$N_{i,f}^H = 2\pi \int_0^R \int_{z_{\rm min}}^{Z} \left[\left(g_1^{i,f}\right)^2 + \left(g_2^{i,f}\right)^2 \right] d\rho dz. \tag{7}$$

Here $z_{\rm min}$ corresponds to the neck position, identified as the point between $-Z$ and Z where the nuclear shape $\rho(z)$ has a minimum. We therefore assume that the rupture always occurs where the neck is the thinnest (no random rupture [23]). $[0,R] \times [-Z, Z]$ is the finite numerical domain.

We can now separate the contributions of the light (L) and of the heavy (H) fragments:

$$E^*_{\rm sc}(L, H) = 2 \times \sum_f e_f \left(V_f^2 - v_f^2 \right) N_f^{L,H}, \tag{8}$$

$$\nu_{\rm sc}(L, H) = 2 \times \sum_i v_i^2 \left(1 - \sum_f |a_{if}|^2 \right) N_i^{L,H}. \tag{9}$$

The assumptions made in Eqs. (8) and (9) are quite obvious: (a) if before scission the emitted neutron was in the L (H) fragment, it is emitted from that fragment, and (b) if after scission the excited neutron is in the L (H) fragment, it contributes to the excitation of that fragment.

III. NUMERICAL RESULTS FOR ^{236}U

As mentioned in the Introduction, it is necessary to know the excitation energy of each fission fragment in order to simulate their deexcitation by neutron evaporation and γ-ray emission. In this section results for two out of the three terms of this energy are presented, namely, for the energy cost to promote neutrons into the continuum $E_{\nu sc}$ and for the excitation energy of the rest of the neutrons E^*_{sc}. Both terms are caused by the nonadiabatic transition at scission. The neutrons are promoted to higher-energy states lying above and below zero, respectively. Contrary to E^*_{sc}, which is entirely used to evaporate neutrons, the fate of $E_{\nu sc}$ is more complicated due to the possible reabsorption of the scission neutrons. As shown in the previous section, our microscopic scission model can calculate these two terms for each individual fragment.

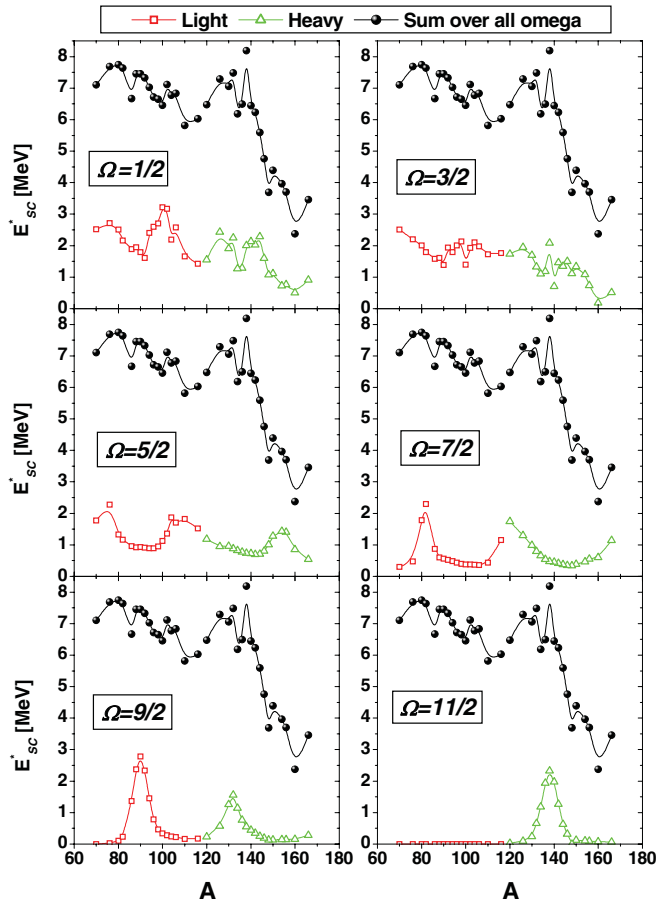

FIG. 1. (Color online) Contributions of each set Ω of neutron eigenstates to the excitation energy at scission (as well as the integral results, solid circles) as a function of the primary-fragment mass. The solid line is an eye-guiding spline interpolation through the calculated points.

A. Excitation energy at scission

The stationary Schrödinger equation is always solved for a given value of Ω at a time and this is also how the results are presented here. Each frame in Fig. 1 represents E^*_{sc} for a given set of eigenstates together with the integral result (summed over all Ω values). In this way one can see the relative contribution of each set and its distribution over fragment masses. In most cases the L fragment is more excited than the H fragment. However, $\Omega = 11/2$ is an exception because there is only one state below the Fermi level; it is entirely located in the H fragment and its energy increases from α_i to α_f. It leads to an exceptionally large excitation in a narrow interval of H masses. Furthermore, $\Omega = 9/2$ is in an intermediate situation. There is one narrow mass interval with high excitation in each of the L and the H fragment regions. For $\Omega = 7/2$ the values are small at the peak of the mass distribution and have therefore little contribution to E^*_{sc}.

The integral curve shows more excitation energy in the L fragments than in the H fragments. If we substract the $\Omega = 11/2$ contribution (which is somewhat abnormal) this feature appears more clearly as one can see in Fig. 2 where the sum $E^*_{sc}(H) + E^*_{sc}(L)$ is also plotted. It is 12 MeV on the average and it decreases from symmetric to asymmetric fission.

The "experimental" excitation energy at scission was repeatedly inferred from the magnitude of the proton even-odd effect [24–28]. Although different, all prescriptions converge toward a 6-MeV upper limit. The present model predicts less excitation energy for protons than for neutrons: due to their electrostatic interaction protons are less present in the neck region where the drastic potential change takes place. Hence our 12 MeV (also an upper limit) for neutrons is not in contradiction with 6 MeV for protons. This difference could explain a smaller even-odd effect for neutrons than for protons [25]. The usual explanation is however the prompt-neutron evaporation that removes the primary effect. Another

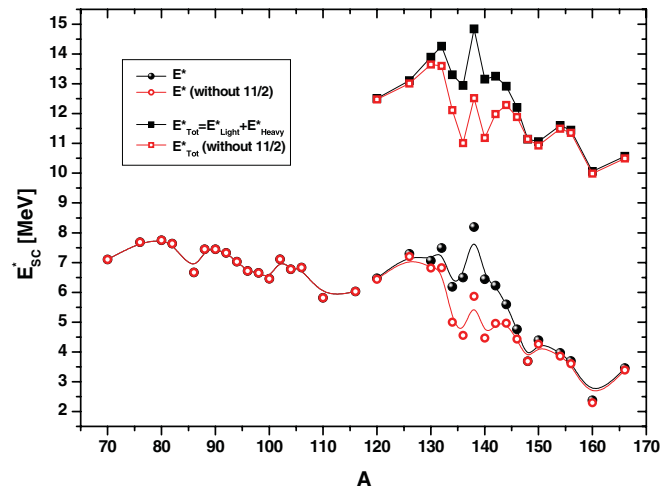

FIG. 2. (Color online) Contribution of the $\Omega = 11/2$ bound state to the excitation energy at scission (circles) and to the excitation energy of each fragment pair ($L + H$) (squares) as a function of the primary-fragment mass. A spline approximation to the calculated points is added to guide the eye.

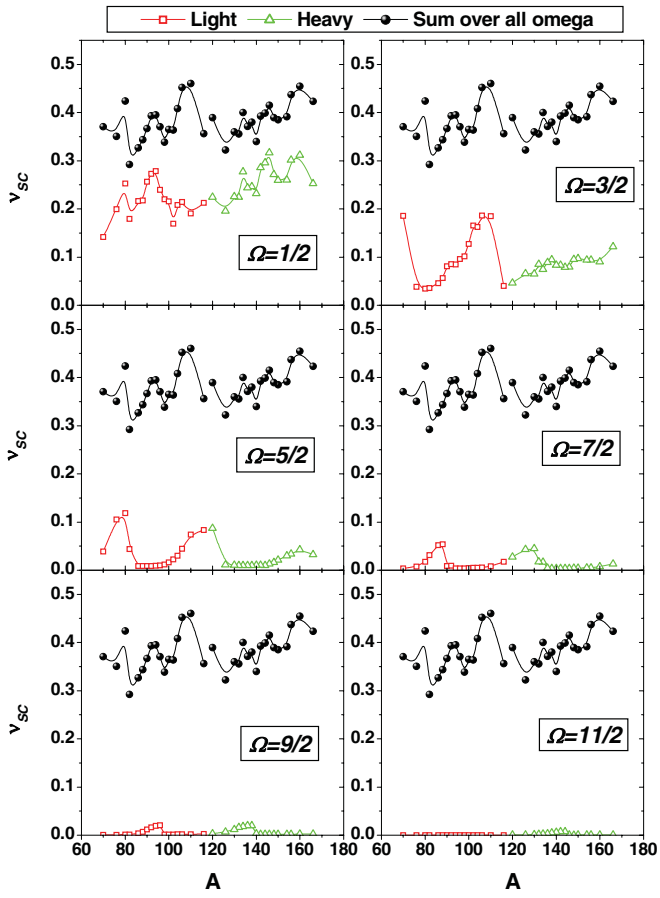

FIG. 3. (Color online) The same as in Fig. 1 but for the scission neutron multiplicity.

type of analysis [29] leads to a 15-MeV upper limit of the excitation at scission for protons and neutrons combined. It compares total kinetic energy (TKE), neutron, and γ-ray data for ^{252}Cf(sf) with a calculated potential energy at scission.

The average experimental TXE in ^{235}U($n_{\rm th}$,f) is 23 MeV [30]. It means that, according to our calculations, at least 50% of it is accumulated during scission.

B. Scission neutron multiplicity

The multiplicity of unbound neutrons at scission $\nu_{\rm sc}$ is represented in Fig. 3. Contrary to $E^*_{\rm sc}$, where the contributions of different Ω are comparable, $\nu_{\rm sc}$ is drastically decreasing with increasing Ω. The trend of the integral value is also different: on the average $\nu_{\rm sc}$ slightly increases with the primary-fission-fragment mass A. A similar increase of $\nu_{\rm sc}$ with the neutron number was observed in a series of Pu isotopes [31]. It is interesting to note that, except maybe for $\Omega = 11/2$, all other cases exhibit a sawtooth structure.

C. Energy cost

We expect only few of these unbound neutrons (namely those moving perpendicular to the fission axis) to leave the fragments without interacting. The others will be scattered or

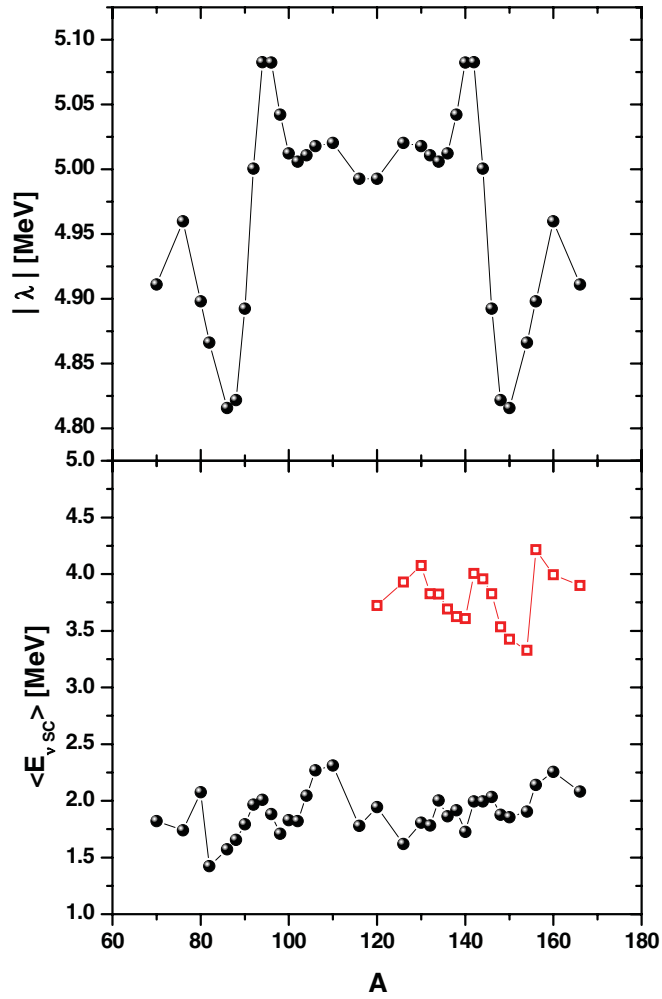

FIG. 4. (Color online) Energy cost to promote neutrons to unbound states at scission (lower panel) and position of the Fermi level λ (upper panel) as a function of the primary-fragment mass.

reabsorbed. Preliminary calculations of this n-FF interaction using a simplified optical model are reported in Ref. [22]. When the scission neutrons are reabsorbed they give back the energy that was used to bring them into the continuum. More precisely the energy is distributed through collisions among other nucleons and contributes in this way to the excitation energy of the primary fragments. At the limit of complete reabsorption, this energy is given by Eq. (5) and is represented in Fig. 4 (bottom panel) as a function of the fragment mass. It is the second scission term in TXE. One of the factors, $|\lambda|(A)$ [32] is also plotted (top panel of Fig. 4). It shows a jump at the most probable mass division 95/141 as it should. Stable configurations are stronger bound and therefore have higher values of $|\lambda|$. However, relative to the other factor $\nu_{\rm sc}$(A), this jump is too weak to show up in $\langle E_{\nu{\rm sc}}\rangle$(A).

D. Temperature at scission

It is now useful to examine the nature of the single-particle excitations produced during the sudden transition at scission in order to see if the situation is close to equilibrium or

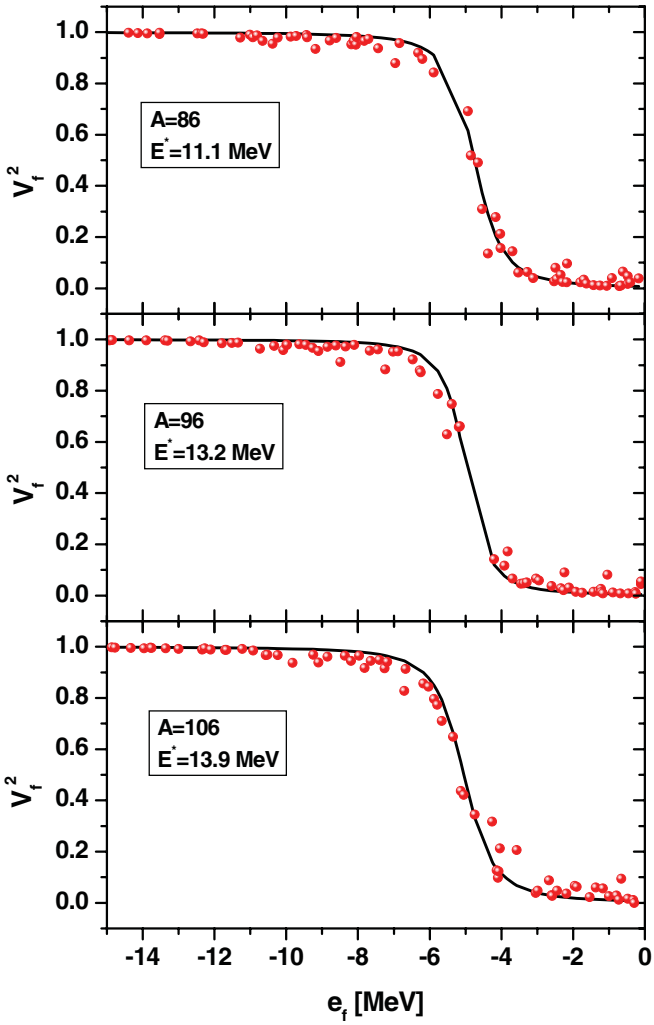

FIG. 5. (Color online) Occupation probabilities of bound neutron-states immediately after scission compared with ground-state probabilities.

not. In Fig. 5 are plotted the occupation probabilities of all bound neutron states in the α_f configuration for selected mass divisions ($A_L = 86$, 96, and 106). The ground-state BCS occupation probabilities, which resemble an equilibrated situation, are also shown for comparison. It is clear that, in our model, the fission fragments at scission are not in thermal equilibrium. However, in the field of fission-neutron emission, one always refers to the temperature of the primary fragments. For this reason it is interesting to see what values of T correspond to $E^*_{\rm sc}$, once thermalized:

$$T_{\rm sc}(L, H) = \sqrt{E^*_{\rm sc}(L, H)/a}. \qquad (10)$$

After scission the shape of the fragments are continuously changing and it is legitimate to ask what level-density parameter to use and to what deformation should it correspond.

According to the schematic Fig. 9 of Ref. [33] the relaxation of the primary-fission-fragment shape occurs much before the complete acceleration, namely, when the fragments attain only 30% of TKE. Combining this information with two-point charge trajectory calculations [34] one deduces a shape

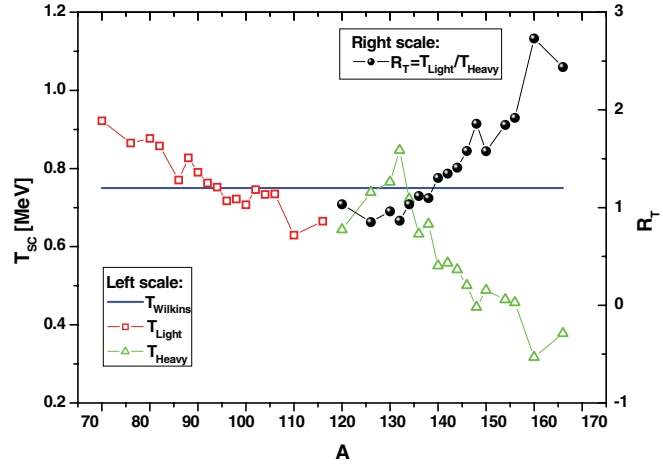

FIG. 6. (Color online) Temperature of the L and H fragments (left scale) induced by the excitation energy at scission and their ratio (right scale) as a function of the fragment mass. The experimental value [40] is also plotted for comparison (solid line).

relaxation time of the order 5×10^{-22} s. This estimate is valid for weak to moderate damping. With a time between collisions of $T = \hbar/2W_0 = 1.1 \times 10^{-22}$ s [35] and five collisions to attain thermal equilibrium, one arrives at a thermalization time comparable with the relaxation time. The depth of the imaginary potential $W_0 = -3$ MeV [36] is the mean of the surface and the volume terms for neutrons with an average kinetic energy of 22 MeV (according to the Fermi gas model [37]).

There is, however, no experimental information on the relaxation time immediately after scission to test the value deduced above. If nevertheless the thermalization is slower than the shape relaxation, it makes sense to use ground-state level-density parameters [38]:

$$a = \overline{a}\left\{1 + \frac{\delta W}{U^*}(1 - e^{-\gamma U^*})\right\}, \qquad (11)$$

where $U^* = E^*_{\rm sc} - \Delta$, $\overline{a}(A) = 0.0959A + 0.1468A^{2/3}$, $\gamma = 0.325A^{-1/3}$, δW are taken from Ref. [39], and $\Delta = 12A^{-1/2}$. In this case the resulting temperatures are those displayed in Fig. 6. Except around symmetric fission, they strongly decrease with A. Consequently the ratio $R_T = T_L/T_H$ is close to 1 at symmetry and increases with the mass asymmetry. The calculated temperatures happen to agree with the average temperature at scission extracted from the experimental mass distribution [40]. In Eq. (10) we did not add $E_{\nu \rm sc}$ to $E^*_{\rm sc}$ due to the uncertainty about the reabsorption process. Therefore Fig. 6 is for zero reabsorption.

IV. SUMMARY AND CONCLUSIONS

The partition of the excitation energy between the primary fission fragments at scission is calculated in the framework of a shell-model approach for extreme nuclear deformations. It is therefore consistent with, and the continuation of, the usual way we treat the entire fission process from the ground state to the last saddle point [41].

Two quantities that influence the excitation energy available immediately after scission are selected: the single-particle excitation of the fragments produced during the neck rupture, E^*_{sc}, and the energy used to release scission neutrons and eventually emit them, $E_{\nu sc}$. Due to the partial reabsorption of the scission neutrons by the fragments, a part of $E_{\nu sc}$ contributes to the excitation energy of the primary fragments. This part is presently unknown.

The dependence on the fission-fragment mass ($A = 70$ to 166) is studied for subsets of neutron states characterized by a given projection of the angular momentum ($\Omega = 1/2$ to $11/2$). Different Ω values show indeed different behaviors. The scission neutron multiplicity ν_{sc} has a sawtooth structure at low Ω and is negligible at high Ω. E^*_{sc} tends to decrease with A at low Ω but has contributions only in a narrow mass range at high Ω. The integral values (summed over all Ω's) have the following general trend: E^*_{sc} decreases and ν_{sc} increases with A. Finally, the temperature at scission is extracted as a function of A in the limit of zero reabsorption of the scission neutrons.

ACKNOWLEDGMENTS

One of the authors (N.C.) would like to thank the European Commission for a Grantholder contract. This work was supported in part by Projects PN-II-ID-PCE-2011-3-0049 and PN-II-ID-PCE-2011-3-0554 of the Romanian Ministry of Education and Research.

[1] D. G. Madland and J. R. Nix, Nucl. Sci. Eng. **81**, 213 (1982).
[2] T. Oshawa, in IAEA Report No. INDC(NDS)-251, 1991, p. 71.
[3] S. Lemaire, P. Talou, T. Kawano, M. B. Chadwick, and D. G. Madland, Phys. Rev. C **72**, 024601 (2005).
[4] A. Tudora, Ann. Nucl. Energy **33**, 1030 (2006).
[5] J. Randrup and R. Vogt, Phys. Rev. C **80**, 024601 (2009).
[6] O. Litaize and O. Serot, Phys. Rev. C **82**, 054616 (2010).
[7] P. Talou, B. Becker, T. Kawano, M. B. Chadwick, and Y. Danon, Phys. Rev. C **83**, 064612 (2011).
[8] N. Carjan, P. Talou, and O. Serot, Nucl. Phys. A **792**, 102 (2007).
[9] I. Halpern, in *First Symposium on Physics and Chemistry of Fission* (IAEA, Vienna, 1965), Vol. II, p. 369.
[10] M. Rizea and N. Carjan, in *Proceedings of the Scientific Workshop on Nuclear Fission Dynamics and the Emission of Prompt Neutrons and Gamma Rays, 27–29 September 2010, Sinaia, Romania*, edited by F.-J. Hambsch and N. Carjan (Publications office of the European Union, Luxembourg, 2011), p. 123.
[11] N. Carjan and M. Rizea, Phys. Rev. C **82**, 014617 (2010).
[12] K.-H. Schmidt and B. Jurado, Phys. Rev. Lett. **104**, 212501 (2010).
[13] B. B. Singh, S. K. Patra, and R. K. Gupta, Phys. Rev. C **82**, 014607 (2010).
[14] K.-H. Schmidt and B. Jurado, Phys. Rev. C **83**, 061601(R) (2011).
[15] M. Rizea, V. Ledoux, M. Van Daele, G. Vanden Berghe, and N. Carjan, Comput. Phys. Commun. **179**, 466 (2008).
[16] V. S. Stavinsky, N. S. Rabotnov, and A. A. Seregin, Yad. Fiz. **7**, 1051 (1968).
[17] V. V. Pashkevich, Nucl. Phys. A **169**, 275 (1971).
[18] A. J. Sierk, S. E. Koonin, and J. R. Nix, Phys. Rev. C **17**, 646 (1978).
[19] V. M. Strutinsky, N. Ya. Lyashchenko, and N. A. Popov, Nucl. Phys. **46**, 639 (1963).
[20] A. A. Seregin, Yad. Fiz. **55**, 2639 (1992).
[21] F. A. Ivanyuk and K. Pomorski, Phys. Rev. C **79**, 054327 (2009).
[22] T. Wada, R. Nishioka, and T. Asano, in *Proceedings of the Scientific Workshop on Nuclear Fission Dynamics and the Emission of Prompt Neutrons and Gamma Rays, 27–29 September 2010, Sinaia, Romania*, edited by F.-J. Hambsch and N. Carjan (Publications office of the European Union, Luxembourg, 2011), p. 163.
[23] U. Brosa, S. Grossmann, and A. Muller, Phys. Rep. **197**, 167 (1990).
[24] A. Ruben, H. Marten, and D. Seeliger, Z. Phys. A **338**, 67 (1991).
[25] F. Gönnenwein, in *The Nuclear Fission Process*, edited by C. Wagemans (CRC Press, Boca Raton, FL, 1991), Chap. 8, p. 287.
[26] G. Mantzouranis and J. R. Nix, Phys. Rev. C **25**, 918 (1982).
[27] H. Nifenecker *et al.*, Z. Phys. A **308**, 39 (1982).
[28] F. Rejmund, A. V. Ignatyuk, A. R. Junghans, and K.-H. Schmidt, Nucl. Phys. A **678**, 215 (2000).
[29] V. S. Ramamurthy, M. Prakash, and S. S. Kapoor, Phys. Rev. C **21**, 752 (1980).
[30] K. Nishio, Y. Nakagome, H. Yamamoto, and I. Kimura, Nucl. Phys. A **632**, 540 (1998).
[31] N. Carjan and H. Goutte, Phys. At. Nucl. **70**, 1639 (2007).
[32] N. Carjan, M. Rizea, and V. Pashkevich, AIP Conf. Proc. **1238**, 313 (2010).
[33] W. J. Swiatecki and S. Bjornholm, Phys. Rep. C **4**, 325 (1972).
[34] H.-H. Knitter, U. Brosa, and C. Budtz-Jorgensen, in *The Nuclear Fission Process*, edited by C. Wagemans (CRC Press, Boca Raton, FL, 1991), Chap. 11, p. 497.
[35] A. Bohr and B. R. Mottelson, *Nuclear Structure* (World Scientific, Singapore, 1998), Vol. I, Chap. 2, p. 214.
[36] A. J. Koning and J.-P. Delaroche, Nucl. Phys. A **713**, 231 (2003).
[37] A. Bohr and B. R. Mottelson, *Nuclear Structure* (World Scientific, Singapore, 1998), Vol. I, Chap. 2, p. 141.
[38] A. V. Ignatiuk, G. N. Smirenkin, and A. S. Tishin, Sov. J. Nucl. Phys. **21**, 255 (1975).
[39] W. D. Myers and W. J. Swiatecki, Nucl. Phys. A **601**, 141 (1996).
[40] B. D. Wilkins *et al.*, Phys. Rev. C **14**, 1832 (1976).
[41] M. Brack, J. Damgaard, A. S. Jensen, H. C. Pauli, V. M. Strutinsky, and C. Y. Wong, Rev. Mod. Phys. **44**, 320 (1972).